

Kinematically-Stabilized Microbubble Actuator Arrays

Guang Yuan¹, Xiaosong Wu², Yong-Kyu Yoon¹, and Mark G. Allen¹

Schools of Electrical and Computer Engineering¹ and Polymer Textile and Fiber Engineering²

Georgia Institute of Technology, Atlanta, GA 30332, USA

Telephone: 1-404-894-9419 Fax: 1-404-894-2776 Email: mallen@ece.gatech.edu

ABSTRACT

A mass-manufacturable endoskeletal micro bubble actuator has been developed and characterized. These pneumatically-actuated devices combine the desirable large deflections of balloon-type actuators with the preferentially-axial deflection of bellows type actuators to produce actuators capable of large deflections in axial directions. This kinematic stabilization is achieved by use of integrated “skeletons” – structures to support desired deflections and suppress unwanted deflections, which underlie the actuator “skin” – elastic structures to help the extended actuator recoil to its original shape. The actuators have been fabricated and characterized, as well as compared with pure-bubble actuators (skin only) and pure-bellows actuators (skeleton only) of the same materials and dimensions. Pure-bubble actuators demonstrated unwanted omni-directional inflation. Pure-bellows actuators demonstrated unstable and irreversible deformation during extension. In contrast, endoskeletal microbubble actuators of 2.6 mm diameter have achieved reversible axial extensions of approximately 0.9mm.

Keyword: digital clay, endoskeletal membrane, inclined exposure, micro bubble actuator

1. INTRODUCTION

Research into endoskeletal corrugated micro bubble actuators is motivated by its application in “Digital Clay” – a two- or three-dimensional haptic computer interface that will enable both user-specified display of shapes as output from a computer and the user-directed input of shapes to a computer [1]. Essentially, digital clay can be thought of as a touch-based, distributed, input or display device. Actuators for digital clay must possess the following attributes: (1) ability to generate large deflections for tactile input/output; (2) ability to generate large forces to interact with human input; and (3) ability to be mass-manufacturable so large arrays can be inexpensively formed. One approach that possesses these attributes is a MEMS-compatible, hydraulically or pneumatically driven, microbubble actuator array. In this approach, the surface of the Digital Clay will be defined by an actuated kinematic structure, the actuators of which are the microbubbles. In other words, each

individual microbubble actuator will form a tactile ‘pixel’ in the digital clay structure.

Previously, several pneumatic microactuators fabricated by MEMS technology have been reported. Among them, micro balloons made of elastomer such as silicone rubber or polyurethane have the advantages of a relatively simple structure and fabrication sequence while simultaneously being capable of large deflection as shown in Figure 1a. These actuators have been used in end-effectors [2], acoustic impedance control [3], and aerodynamic control [4]. However, balloons typically deflect omni-directionally, making linear actuation such as that desired in the digital clay application more difficult. Furthermore, the non-monotonic pressure-radius relation for a balloon suggests stability problems may occur when a pure balloon actuator is either intentionally or accidentally hyper-inflated. Modifications to traditional balloon actuators are therefore required to achieve large, stable deflections in certain preferential directions.

Alternatively, a corrugated diaphragm made of non-elastomeric, relatively high modulus material can be used to achieve a preferentially-axial deflection as shown in Figure 1b. Corrugated diaphragms are widely used in altimeters, pressure gauges, speakers, or other applications in which large linear deflections are required. They are usually built using a high precision

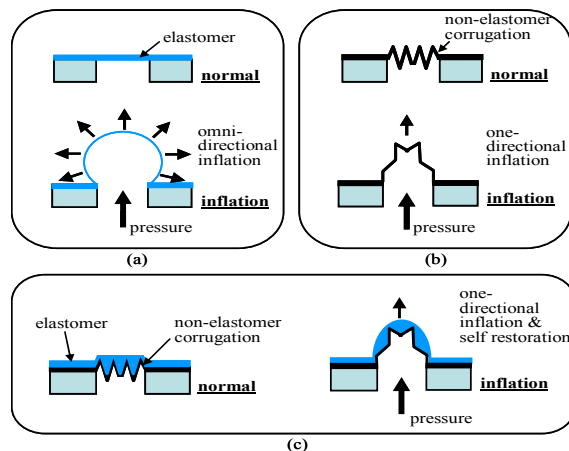


Figure 1. Various microbubble membranes: (a) elastomeric membrane, (b) non-elastomer-based corrugated membrane, (c) endoskeletal membrane

mold/die made through traditional mechanical methods, which are not suitable for mass-manufacturing. In addition, the membrane shows often a poor self-restoration property when the diaphragm is hyperextended, e.g., inflated to its full extent. When this occurs, the diaphragm can reach a local stability point, not returning to the original position even after removal of the external pressure.

In this paper, we present a mass-manufacturable endoskeletal micro bubble actuator capable of reversible vertical deflection. In our approach, micro corrugated non-elastomeric (polyarylene) diaphragms are embedded under soft elastomer (polyurethane) membranes during the fabrication process to form a skeleton as shown in Figure 1c. The corrugated shape of the skeleton defines the deflection to be primarily in the desired direction. The elastomer acts to enhance the ‘spring back’ mechanism of the corrugated diaphragm, thereby enhancing the linearity and reversible expansion of the actuator even to the full extent of the corrugations. Applications of this structure extend beyond Digital Clay, and may include passive pressure gauges and sensitive pressure sensors. In our study, the skeletal corrugated sections of the microbubble array were achieved using a single lithographic mask by continuously rotating inclined exposure [5-7] followed by sacrificial material molding and polyarylene coating. This approach to endoskeletal bubble actuators is not only mass-manufacturable, but can also be scaled down to even smaller dimensions if required.

2. DESIGN & FABRICATION

Bellows actuators characteristically have a large linear deflection in their axial direction; an implementation in the vertical dimension using micromachining techniques has been demonstrated [8]. For these vertical devices, however, the fabrication complexity and process time increases as the number of corrugations of the bellows increases. Therefore, corrugated diaphragms are often utilized as an alternative for a micro actuator requiring large vertical deflection. In this research, a combination of triangular and trapezoidal profiles is adopted for the micro corrugations. The slanted sidewalls of the corrugations are achieved using a continuously rotating inclined exposure technique as shown in Figure 2.

A photopatternable negative tone epoxy (SU-8, Microchem, Inc.) is spin-coated on a glass substrate and soft-baked. The substrate is mounted on a rotational stage with an angle θ . A UV mask with concentric circular patterns is placed on the substrate and UV-exposed with an appropriate optical dose in rotational mode (Figure 2a). After post-baking the substrate, the cross-sectional view of A-A' in Figure 2a is shown in Figure 2b. A combination of triangular and trapezoidal profiles is obtained after development. The dimensions

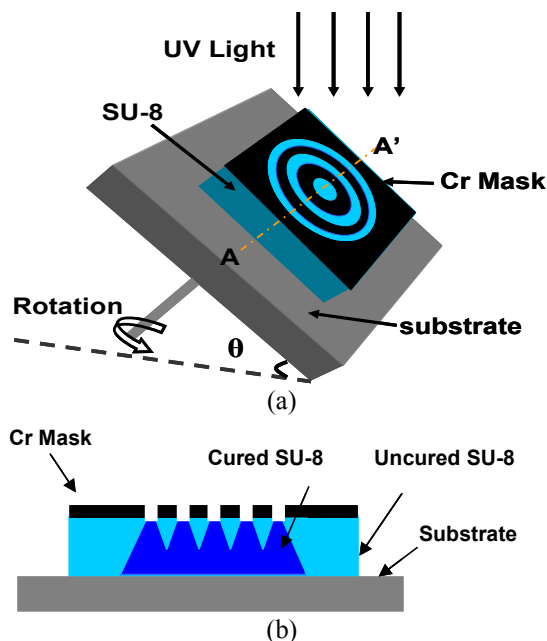


Figure 2. Continuously rotational inclined exposure for concentrically corrugated diaphragm with slanted side walls: (a) exposure scheme, (b) cross-sectional view of A-A'

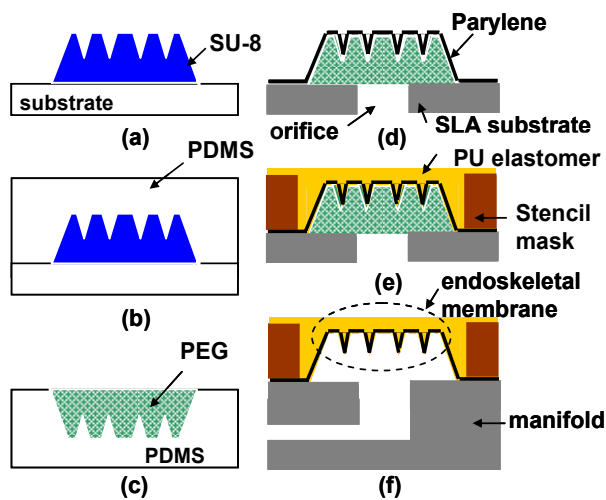


Figure 3. Overall fabrication process

of the corrugations are determined by the width and intervals between two concentric patterns as well as the inclined angle. By increasing the number of concentric circular patterns and increasing the steepness of the slanted side wall, achievable maximum deflection increases, which has the tradeoffs of more difficult mold release in subsequent processing as well as increased susceptibility to mechanical instability. In this research, a corrugation of six concentric patterns and a slanted angle of 30° , with a diameter of 2.6mm, has been chosen.

Figure 3 details the overall fabrication process. A master pattern of corrugated diaphragms is fabricated using SU-

8 as described in the previous section (3a). Polydimethylsiloxane (PDMS, Sylgard 184) is cast onto the SU-8 patterns to obtain a negative replica (3b). After separating the PDMS from the substrate, a sacrificial material (PEG wax, Kindt Collins) is cast into the PDMS mold (3c). The PEG corrugation array is batch-transferred onto an epoxy substrate having a matching orifice array pattern, in which the orifices are aligned with the concentric diaphragms. The epoxy substrate is fabricated by stereo-lithography (SLA). A parylene layer is conformally coated to form the corrugated skeletal membranes (3d). A stencil mask fabricated by SLA is placed on the substrate to level the top surface and a thin layer of polyurethane elastomer (Polytek, Poly 74-20) is then spin-coated on top of the corrugated surface (3e). The elastomer is cured and the sacrificial PEG is removed by dissolving in water to form endoskeletal membranes. The endoskeletal membrane array is bonded to a manifold fabricated by SLA, which enables each actuator to be addressed independently (3f).

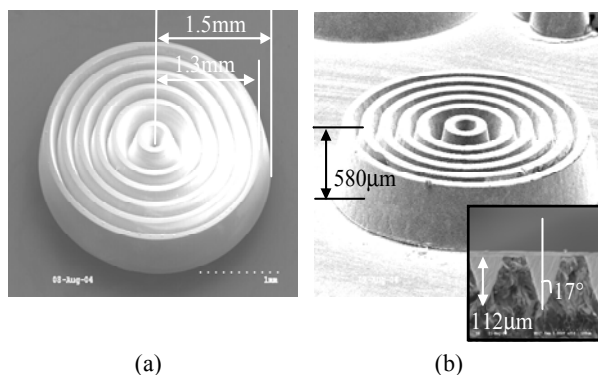


Figure 4. Comparison of (a) SU-8 mold and (b) replicated PEG mold: inset shows a cross-sectional image of corrugation profile

SEM photomicrographs of a single corrugated SU-8 pattern and a corresponding cast PEG pattern replicated from PDMS are shown in Figure 4. The top diameter, the bottom diameter, and the height of the diaphragm are 2.6mm, 3.0 mm, and 580 μm , respectively. An incident angle θ of 30° results in a refracted angle of approximately 17° . Each corrugation has a depth of 112

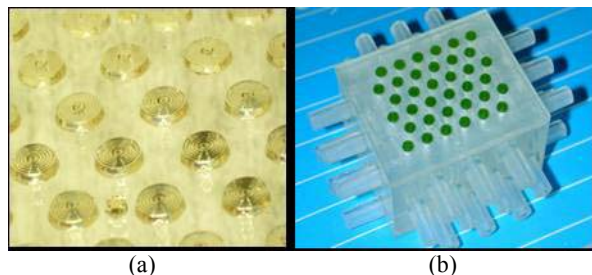


Figure 5. Corrugated pattern array: (a) SU-8 master pattern array, (b) batch-transferred corrugated PEG corrugation array on SLA manifold substrate

μm . It can be seen that the molded PEG structures faithfully follow the original SU-8 micro corrugation. Figure 5a and 5b show an SU-8 micro corrugated mold array and a batch-transferred corrugated PEG mold array mounted on a stereolithography manifold substrate, respectively.

3. TESTING RESULTS

Figure 6 shows inflated and restored shapes for (a) an endoskeletal bubble actuator and (b) a pure-bubble actuator (PU skin-only). For the endoskeletal structure, the inflation of the membrane is observed to be confined to one direction, i.e. out-of plane, and the displacement is a reasonably linear function of the applied pressure. After the applied pressure is removed, the membrane almost returns to its original position and shape. The pure-bubble actuator shows similar stability and one-directional movement with small inflation while the membrane shows an omni-directional balloon-like expansion in large inflation, resulting in plastic deformation of the material. Note that when the membrane is deflated by removing the applied pressure, it becomes flaccid and does not return to its original shape.

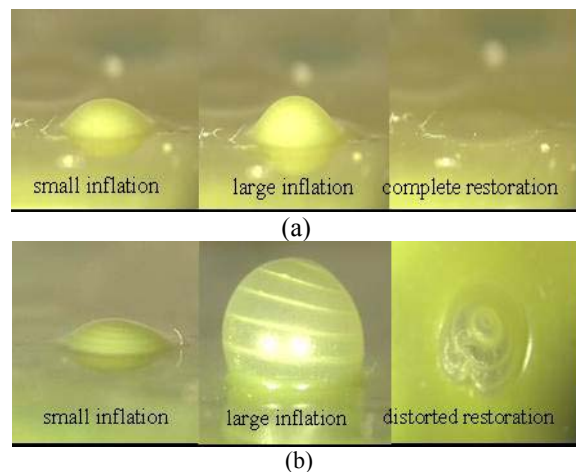


Figure 6. Shape comparison of (a) endoskeletal bubble and (b) pure-bubble

Membrane deflection as a function of applied pressure has been quantitatively characterized as shown in Figure 7. Compressed air is applied to the membrane through the manifold channels and membrane displacement is measured using a microscope equipped with an xyz-stage. For comparison, three actuators are fabricated and tested: a pure-bubble actuator (PU skin-only), a pure-bellows actuator (parylene skeleton-only), and an endoskeletal actuator (composite of PU skin and parylene skeleton). In Figure 7, although the pure-bellows (parylene skeleton-only) actuator shows a maximum deflection of up to 1.9 mm with full extension of the corrugations, the deflection is irreversible due to instability of the hyper-extended bellows. This irreversibility manifests itself as distinct ‘jumps’ in the

pressure-deflection curve as each corrugation ‘unfolds’ and does not ‘refold’ upon release of pressure. Addition of elastomer greatly enhances the membrane stability in the pressure-deflection characteristics of the endoskeletal bubbles, maintaining the unidirectional deflection of the actuator. It should be noted that the actuators in Figure 7 exhibit typical viscoelastic responses with hysteretic behavior during inflation and deflation.

Among the three comparison actuators, the pure-bubble actuator has an extremely low modulus and requires the smallest pressure to achieve a given deflection. The endoskeletal bubbles require the largest pressure for the same deflection because they consist of a composite of two materials: polyurethane (PU) and parylene, each layer of the composite possessing the same thickness as the other two bubble actuators, thereby resulting in the largest effective stiffness. To verify these observations, numerical analysis of each actuator is performed using ANSYS and the experimental results are compared with the simulation. The calculated displacements as a function of pressure agree well with the experimental data for small deflection in all three cases, as can be seen in Figure 8.

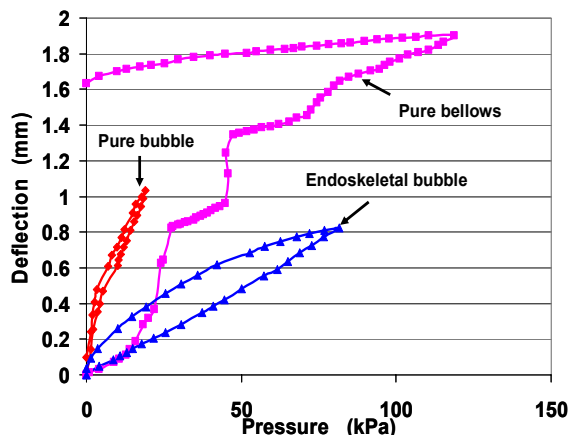


Figure 7. Membrane deflection as a function of applied pressure for three actuators: a pure-bubble actuator, a pure-bellows actuator, and an endoskeletal bubble actuator

4. CONCLUSION

A hydraulically driven, kinematically stabilized endoskeletal bubble actuator has been proposed and implemented for future use in digital clay research. The actuator has been fabricated using the mass-manufacturable approaches of lithography and micromolding. The skeletal corrugated sections have been fabricated by using continuous rotating inclined exposure. Micro pure-bubble (PU skin-only) and pure-bellows bubbles (parylene skeleton-only) with the same profiles have also been fabricated and characterized for

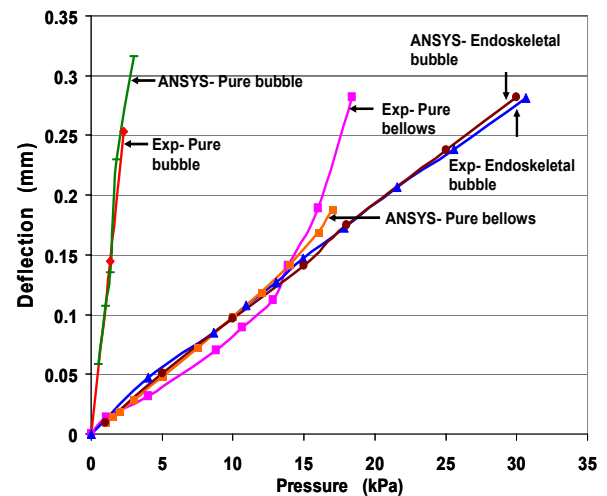


Figure 8. Comparison of experimental and finite element results for all three actuator types in small deflection.

purposes of comparison. The endoskeletal bubble actuator demonstrated stable, directional deflection as a function of applied pressure, and was well-characterized by appropriate finite-element modeling.

REFERENCES

- [1] J. Rossignac, M. Allen, W.J. Book, and A. Glezer, “Finger sculpting with Digital Clay: 3D shape input and output through a computer-controlled real surface,” *Proceedings of International Shape Modeling Conference, 2003*, May 12-15, 2003, pp. 229-231.
- [2] F. Kawai, P. Cusin, and S. Konishi, “Thin flexible end-effector using pneumatic balloon actuator,” *Proceedings of IEEE Micro Electro Mechanical Systems, 2000*, pp. 391-396.
- [3] C. Grosjean, G.B. Lee, W. Hong, Y.C. Tai, and C.M. Ho, “Micro Balloon Actuators for Aerodynamic Control”, *Proceedings of IEEE Micro Electro Mechanical Systems, 1998*, pp. 166-171.
- [4] M. Yoda and S. Konishi, “Acoustic impedance control through structural tuning by pneumatic balloon actuator”, *Proceedings of IEEE Micro Electro Mechanical Systems, 2001*, pp. 244-247.
- [5] Y.-K. Yoon, J.-H. Park, F. Cros, and M.G. Allen, “Integrated vertical screen microfilter system using inclined SU-8 structures,” *Proceedings of IEEE Micro Electro Mechanical Systems, 2003*, pp. 227-230.
- [6] M. Han, W. Lee, S.-K. Lee, and S.S. Lee, “Fabrication of 3D microstructures with inclined/rotated UV lithography,” *Proceedings of IEEE Micro Electro Mechanical Systems, 2003*, pp. 554-557.
- [7] K.-Y. Hung, H.-T. Hu, and F.-G. Tseng, “Application of 3D glycerol-compensated inclined-exposure technology to an integrated optical pick-up head,” *J. Micromech. Microeng.* vol. 14 (2004) 975–983.
- [8] X. Yang; Y.-C. Tai; and C.-M. Ho; “Micro Bellow Actuators”, *International Conference on TRANSDUCERS '97*, vol. 1, pp.45-48.